Journal of proteome research

Article

pubs.acs.org/jpr

Quantitative NMR Metabolite Profiling of Methicillin-Resistant and Methicillin-Susceptible *Staphylococcus aureus* Discriminates between Biofilm and Planktonic Phenotypes

Mary Cloud B. Ammons,*[,†] Brian P. Tripet,[†] Ross P. Carlson,[‡,§] Kelly R. Kirker,[§] Michael A. Gross,[†] Jessica J. Stanisich,[†] and Valérie Copié*[,†]

[†]The Department of Chemistry and Biochemistry, [‡]Department of Chemical and Biological Engineering, and [§]The Center for Biofilm Engineering, Montana State University, Bozeman, Montana 59717, United States

ABSTRACT: Wound bioburden in the form of colonizing biofilms is a major contributor to nonhealing wounds. *Staphylococcus aureus* is a Gram-positive, facultative anaerobe commonly found in chronic wounds; however, much remains unknown about the basic physiology of this opportunistic pathogen, especially with regard to the biofilm phenotype. Transcriptomic and proteomic analysis of *S. aureus* biofilms have suggested that *S. aureus* biofilms exhibit an altered metabolic state relative to the planktonic phenotype. Herein, comparisons of extracellular and intracellular metabolite profiles detected by ^{1}H NMR were conducted for methicillin-resistant (MRSA) and methicillin-susceptible (MSSA) *S. aureus* strains grown as biofilm and planktonic cultures. Principal component analysis distinguished the biofilm phenotype from the planktonic phenotype, and factor loadings analysis identified metabolites that contributed to the statistical separation of the biofilm from the planktonic phenotype, suggesting that key features distinguishing biofilm from planktonic growth include selective amino acid uptake, lipid catabolism, butanediol fermentation, and a shift in metabolism from energy production to assembly of cell-wall components and matrix deposition. These metabolite profiles provide a basis for the development of metabolite biomarkers that distinguish between biofilm and planktonic phenotypes in *S. aureus* and have the potential for improved diagnostic and therapeutic use in chronic wounds.

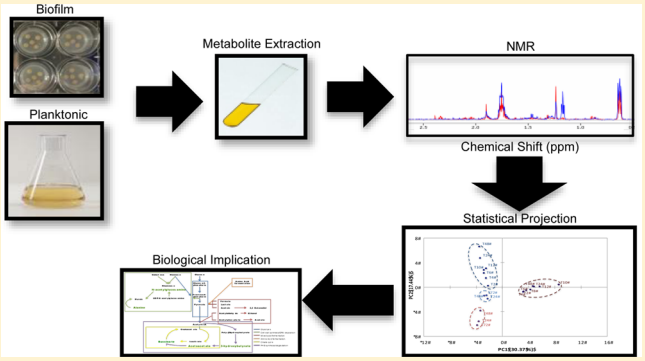

KEYWORDS: *Staphylococcus aureus, biofilm, NMR metabolomics*

INTRODUCTION

An estimated $58 billion in medical costs are associated with chronic wound complications afflicting over 18 million diabetics in the United States;[1] 24% of diabetics can expect to undergo limb amputation within their lifetime as the result of a chronic, nonhealing wound.[2] The social and economic burdens of these types of wounds are severe and growing rapidly.

While chronicity of the wound likely results from multiple factors such as dysfunctional circulation and compromised immunity, wound bioburden in the form of bacterial biofilm is a major contributing factor in the shift from acute to chronic wound.[3] Bacterial biofilms are structured communities of cells that adhere to a surface and display phenotypic heterogeneity.[4] In the case of the wound bed, the surface is biotic with the bacterial biofilm adhering to devitalized tissue. The chronic wound biofilm persists at the solid surface−air interface and is sustained via exudate seeping from the wound, resulting in a complex nutritional environment. Relatively little is known about the metabolism of these bacterial communities and whether there exists potential small molecule biomarkers associated with their metabolism that could be of diagnostic, prognostic, or therapeutic use.

One of the most common, opportunistic, bacterial colonizers found across multiple types of chronic wounds is the Gram-positive *Staphylococcus aureus*, which can be either methicillin-resistant (MRSA) or methicillin-susceptible (MSSA).[5] *S. aureus* is a facultative anaerobe that can grow by utilizing either oxygen or nitrate for respiration or by mixed acid fermentation.[6] Despite the prevalence of *S. aureus* in chronic wounds, the basic physiology of this opportunistic pathogen is still poorly understood,[7] especially with regard to the biofilm phenotype.

Within biofilms, bacterial cells can experience significant environmental heterogeneity,[8] and these microenvironments appear to be related to virulence.[9] It has been postulated that altered metabolism contributes to the higher tolerance of bacterial biofilms to therapeutic agents[10] and, while biofilms have traditionally been regarded as metabolically dormant,[11] recent transcriptomic and proteomic analyses of *S. aureus*

Received: February 5, 2014
Published: April 29, 2014

biofilms indicate that cells within a biofilm have active, though altered, metabolic activity relative to planktonic growth.[9a,12] These investigations are, however, distantly removed from direct detection of phenotype. In contrast, metabolomic analysis of small molecule metabolites present in both the extracellular and intracellular environments provides a more direct assessment of the defining characteristics of cellular phenotype.[13] For example, Zhu and coworkers[14] investigated the role of selective amino acid uptake by biofilms, suggesting that cells within a biofilm do not have ready access to external electron acceptors necessitating organic acid-producing fermentative strategies and that ammonia generation by arginine deiminase enzymatic activity offsets pH decreases due to accumulation of these organic acids. However, mutational analysis demonstrated that arginine deiminase is not essential for *S. aureus* biofilm growth.[14] How selective uptake of amino acids by the biofilm impacts biofilm physiology remains an open question, warranting further investigation.

Correlations between virulence and metabolism have been observed at the transcriptomic, proteomic, and metabolic levels for *S. aureus*[12,14,15] and strain-dependent differences in the biofilm forming capacity of *S. aureus* have been demonstrated, suggesting a correlation between metabolic activity and pathogenicity;[16] however, direct time course comparison of metabolic changes between strains that exhibit different virulence traits and between planktonic and biofilm growth conditions have not been performed. In the present study, we have utilized quantitative ^{1}H NMR spectroscopy to detect and identify both intracellular and extracellular water-soluble small-molecule metabolites. The metabolic profiles of a methicillin-resistant and a methicillin-susceptible *S. aureus* strain, grown both as biofilm and planktonic cell cultures over extended time periods, were characterized. The model biofilm culturing system used here mimics a chronic wound environment by growing the biofilm colonies at a solid surface−air interface with nutrients absorbed from growth media in a fashion similar to biofilms extracting nutrients from seeping exudate of a chronic wound.[17] This culturing strategy is in stark contrast with previous metabolic comparisons between biofilm and planktonic cultures of *S. aureus* that used a closed-system, flow-cell model of biofilm growth, in which oxygen exchange with air is limited.[14]

The ability to readily quantify metabolites confers an advantage to NMR metabolomics[18] and facilitates the use of unsupervised, orthogonal projection-based, statistical analyses such as principal component analysis (PCA).[19] PCA analysis yields insights into metabolic relationships between different bacterial phenotypes without biasing the statistical clustering output of those phenotypes. Using PCA analysis, it was possible to differentiate between pathogenic (MRSA) and nonpathogenic (MSSA) strains of *S. aureus* based on metabolite profiles. In addition, it was possible to distinguish between *S. aureus* biofilm and planktonic phenotypes using PCA analysis of metabolite profiles in a complex growth medium. This study lays the groundwork for assessing the efficacy of therapeutic strategies based on small-molecule targets identified through metabolomics approaches for *S. aureus* biofilm colonization of chronic wounds, while also gaining insights into metabolic strategies that characterize biofilm physiology.

EXPERIMENTAL PROCEDURES

Bacterial Strains, Growth Conditions, and Sampling

Two phylogenetically distinct strains of *S. aureus* were used in this study: the methicillin-resistant (MRSA) clinical wound isolate *S. aureus 10943*[17,20] and the methicillin-susceptible (MSSA) laboratory strain *S. aureus* ATCC 6538.[17,20b,c,21] Growth media for both planktonic and biofilm cultures consisted of tryptic soy broth (TSB) (Fluka Analytical). Inocula for both planktonic and biofilm growth conditions consisted of batch cultures grown in TSB at 37 °C to an optical density reading of 1.7 at 600 nm (OD_{600nm}). Aliquots (1 mL) were collected for serial dilution, drop plating, and calculation of colony forming units (cfu).

For planktonic studies, inoculum cultures were diluted 1:100 in fresh TSB and cultured at 37 °C in 1 L flasks shaking at 150 rpm. Planktonic cultures were grown under aerobic conditions with flask-to-medium volume ratios of 3:1. Cultures (10 mL) of cells and supernatant were harvested every 2 h up to 12 h, then at 24 and 48 h post inoculation. Biofilm growth was cultured as previously described.[17] In brief, tissue culture inserts (Millipore Millicell, 0.4 μm pore size) were inoculated with five 10 uL droplets of overnight inoculum culture (~10^8 cfu/mL) and grown for 72 h at 37 °C, at which point the biofilms had reached linear growth, which is referred to here as the T0 biofilm growth point.[17] Although pore size on the tissue culture insert did not prevent bacterial cells from escaping into the growth medium in the well below, the biofilms constituted the primary growth phenotype for the cultures. To maintain biofilm viability, we refreshed growth media every 24 h. Once biofilms reached linear growth phase (T0), biofilms were collected every 24 h, up to 72 h (referred to as T24, T48, and T72 in the text). For each biofilm growth time point, spent supernatant was collected from the plate well, and biofilms were harvested from the insets by gently pipetting with 1 mL of sterile PBS to dislodge the biofilms and were immediately centrifuged at 4700 rpm for 10 min at 25 °C to pellet the cells. As with planktonic samples, biofilm supernatant and pellet were immediately flash-frozen in liquid nitrogen and stored at −80 °C. In addition, sham controls (i.e., TSB media only with no bacterial inoculation) were included on each plate to assay for leaching of plate materials into media as well as loss of volatile compounds from media due to culture conditions. For all growth conditions, samples were harvested in technical triplicates and repeated in biological duplicates.

NMR Sample Preparation

NMR samples were prepared from duplicate experiments with triplicate technical replicates for each growth condition and each time point. Metabolites were extracted as previously described.[21a,22] Although leakage of intracellular metabolites into the extracellular environment has been reported for certain metabolism quenching procedures,[23] limited loss of organic acids during sample preparation and statistical reliability across methods[21a] indicated that the cold methanol extraction method is most suited for harvesting and extracting metabolites from our samples. In brief, supernatants were filtered through an extensively prewashed centrifuge filter (with sterile-filtered water) with a 3 kDa molecular weight cutoff (Millipore Amicon) prior to lyophylization overnight at room temperature. Cell pellets were washed in 60% ice-cold methanol (Sigma-Aldrich) and centrifuged at 5000 rpm for 10 min. Pellets were resuspended in a 2:1 ice-cold methanol/chloroform solution (Sigma-Aldrich) prior to cell lysis by sonication.

dx.doi.org/10.1021/pr500120c | J. Proteome Res. 2014, 13, 2973−2985

A 1:1 aqueous chloroform solution (Sigma-Aldrich) was added, samples were gently mixed, and aqueous layers were collected by centrifugation and transferred by pipetting to a clean microcentrifuge tube. Aqueous layer samples were lyophilized overnight at room temperature. Lyophilized samples were stored at −20 °C until further use. For ^{1}H NMR, lyophilized samples were resuspended in 500 μL of NMR buffer (10 mM NaH_2PO_4/Na_2HPO_4 containing 0.25 mM 4,4-dimethyl-4-silapentane-1-sulfonic acid [DSS] in 100% D_2O, pH 7) and transferred to 5 mm Wilmad NMR tubes.

NMR Analysis

^{1}H NMR spectra were acquired at 298 K (25 °C) on a Bruker 600-MHz (^{1}H Larmor frequency) AVANCE III solution NMR spectrometer equipped with a SampleJet automatic sample loading system, a 5 mm triple resonance (^{1}H, ^{15}N, ^{13}C) liquid-helium-cooled TCI probe (cryoprobe), and Topspin software (Bruker version 3.2). One-dimensional ^{1}H NOESY experiments were performed using the Bruker supplied noesypr1d pulse sequence with 256 scans, ^{1}H spectral window of 9600 Hz. FIDS were collected in 32K data points, with a dwell time interval of 52 μsec amounting to an acquisition time of ∼1.7 s, using a 2 s relaxation recovery delay between acquisitions and a NOESY mixing time period of 50 ms. Pulse sequence settings were based on standard recommendations by the Chenomx guide for recording 1D ^{1}H NMR spectra of small molecule metabolites.

Spectral processing and analysis was performed using the Chenomx NMR software (version 7.6) (Chenomx). For each sample, NMR spectra were phased and baseline-corrected, and a line broadening function of 0.5 to 1.5 Hz was applied according to recommended Chenomx protocols and previously reported metabolomics analysis methods.[21,24] Variable line broadening was applied to each sample to account for small sample variations in pH and shimming as well as to optimize metabolite identification and quantification. For metabolite identification, the Chenomx small-molecule library for 600 MHz (^{1}H Larmor frequency) magnetic field strength NMR was used, and NMR spectral patterns were fitted for each sample independently. The internal DSS standard was used for quantitation of identified metabolites. This study involved two strains of *S. aureus*, each grown in both the biofilm and planktonic modes of growth, with three growth time points for the biofilm and eight growth time points for the planktonic phenotypes. For each strain and phenotype and time point combination, triplicate experimental replicates were performed; thus for each strain, 66 samples were analyzed resulting in an overall experimental matrix of 132 total samples profiled in duplicate. From the analysis of ^{1}H 1D NMR spectra, an overall number of ∼120 compounds were identified with ∼30 compounds identified per sample spectrum, including many common metabolites such as amino acids, fermentation products, and metabolites of central metabolism. For statistical analysis using PCA, over 120 and 40 identified metabolites were attributed to at least one time point from at least one growth condition, for extracellular and intracellular metabolite samples, respectively. To ensure objective metabolite identification and quantification, multiple operators performed spectral fitting independently, and determination of metabolite concentrations was consistent and comparable between different operators.

To verify metabolite ID, select metabolites of particular interest to the analysis were confirmed using 2D NMR or by spiking in pure standards into samples (when available). 2D ^{1}H−^{1}H total correlation spectroscopy (TOCSY) spectra were acquired using a Bruker supplied dipsi2gpph19 pulse sequence and collected with ^{1}H spectral windows of 7200 Hz, 256 points and 2048 points for digitization of the indirect and direct spectral dimensions, respectively, and a 60 ms TOCSY spin lock mixing period. 2D ^{1}H−^{1}H TOCSY spectra were processed using Topspin software (Bruker version 3.2) and compared with corresponding spectra of pure standards.

Chenometrics and Statistical Analysis

Quantified concentrations of metabolites were normalized to cfu, and averages were calculated across technical replicates prior to 2D PCA.[21b] Comparison of PCA plots was performed on duplicate experiments, and similar clustering patterns were observed. Clustering of metabolite variables by PCA was performed using XLSTAT version 3.1 software (Addensoft) and Pearson correlation. 2D PCA accounted for ∼50% of the total variance, significantly more than the cumulative variance of 30% commonly observed in complex biological systems,[25] supporting the statistical clustering reported here. For each distinct metabolite pattern, the principal components (PCs) that accounted for the largest percentage of the variability were used for visual projection on the scores plots of the segregation of metabolite profiles that distinguished growth phenotypes in PCA scores plots.

For each PC, the correlation coefficient of the factor loadings and the square of the cosine of the variable were calculated to identify compounds that most significantly contributed to the separation of the different samples and to establish how significantly a given metabolite variable is correlated to the axis of the principal component (i.e., PC1, PC2). A mathematical rule of thumb is that a factor loading is significant if the correlation coefficient is 0.7 or higher because this accounts for over half of the observed variance; however, in biological systems, the threshold of 0.4 is more commonly used[19] and has been used here. While a correlation coefficient signifies the contribution of a metabolite to a statistical grouping of a given phenotype, the square of the cosine indicates which metabolites are most statistically related to the PCs used to build 2D PCA scores plots. While the factor analysis tables indicate which metabolites most significantly contribute to the separation of samples, they do not represent either positive or negative fold changes in concentrations across samples; therefore, representative, statistically significant fold changes in concentration for metabolites involved in metabolic pathways that most distinguished biofilm and planktonic cultures from a single representative experiment were calculated separately and plotted relative to the concentration of metabolites identified and quantified in the planktonic exponential growth stage. Representative fold changes in select metabolites were calculated using two-tailed unpaired *t* tests and considered significant at $p < 0.05$ using the XLSTAT software plug-in to EXCEL (Addinsoft, version 3.01).

RESULTS

Separation of MRSA and MSSA *S. aureus* Strains Based on Metabolite Profiles

Two phylogenetically distinct strains of *S. aureus* were grown under identical planktonic and biofilm conditions over time courses to comprehensively quantify metabolic differences between planktonic and biofilm phenotypes. *S. aureus 10943* is a community-acquired, methicillin-resistant (CA-MRSA) clin-

dx.doi.org/10.1021/pr500120c | J. Proteome Res. 2014, 13, 2973−2985

ical isolate from a chronic wound.[17,20b,c] For comparison, the common, nonvirulent methicillin-susceptible (MSSA) laboratory strain *S. aureus 6538* (Rosenbach) was also investigated. Phylogenetic separation of these two strains demonstrates that each strain inhabits distinct branches of the *S. aureus* genetic family tree and exhibits distinct degrees of virulence. *S. aureus 10943* most closely aligns with CA-MRSA strain *S. aureus USA300 TCH1516* as well as related MRSA strains such as *S. aureus USA300 FPR3757* and *S. aureus TW20*. *S. aureus 6538* most closely clusters phylogenetically to a related *S. aureus* Rosenbach strain, *S. aureus ATCC 51811*, as well as the MSSA laboratory strain *S. aureus Newman* (Figure 1A).[26]

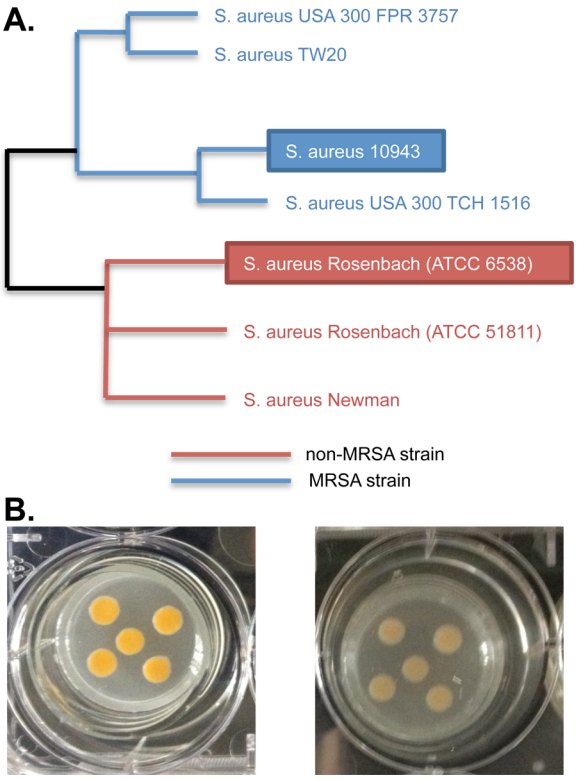

Figure 1. Two phylogenetically distinct strains of *S. aureus* have unique pigmentation. (A) Phylogenetic separation of *S. aureus 6538* and *S. aureus 10943* indicates that *S. aureus 10943* is most closely related to common CA-MRSA strains, while *S. aureus 6538* is most closely related to non-MRSA strains. Blue lines indicate phylogenetic branches associated with methicillin resistance and red lines indicate phylogenetic branches associated with *S. aureus* species with no known antibiotic resistance. Black lines indicate parent phylogenetic branches.[26] (B) Two phylogenetically dissimilar strains of *S. aureus* were inoculated onto tissue culture inserts and grown as biofilms in six-well tissue culture plates at 37 °C. Every 24 hours, feeder medium was refreshed within the plate well. Images represent mature biofilms that have been cultured a total of 72 h to reach linear growth phase (referred to as the T0 biofilm growth time point). Left panel depicts the chronic wound isolate, MRSA strain *S. aureus 10943* and right panel depicts the lab-adapted, MSSA strain *S. aureus "Rosenbach" ATCC 6538*.

The two strains exhibited similar growth profiles. The planktonic cultures were grown under aerobic batch conditions in nonmodified TSB at 37 °C in 1 L shaking flasks. The biofilms were grown in an aerobic-modified tissue culture model that mimics growth conditions found in a chronic wound.[17,20d] While no visible growth differences between the strains were observed in the planktonic cultures, distinct pigmentation differences were noticeable in the biofilm cultures (Figure 1B). Pigmentation in *S. aureus* has been correlated to virulence.[27] Thus, the observable difference in biofilm pigmentation between the strains (Figure 1B, right and left panels, respectively) corroborates with the known clinical significance of *S. aureus 10943* as a MRSA strain.

Growth profiles for *S. aureus 10943* and *S. aureus 6538* batch cultures grown in TSB were similar based on optical density ($OD_{600\ nm}$) readings (Figure 2A) and transitioned through the growth phases at very similar rates, that is, exhibiting exponential growth between 2 and 6 h, transitioning to stationary phase between 8 and 10 h and maintaining stationary phase through the 48 h experimental time course. *S. aureus 10943* and *S. aureus 6538* biofilm cultures also exhibited very similar growth profiles with slightly higher optical densities ($OD_{600\ nm}$) for *S. aureus 6538* biofilm at all time points; however, this $OD_{600\ nm}$ difference was not statistically significant. The $OD_{600\ nm}$ readings for all biofilm time points suggested the biofilms reached a linear growth phase beginning at the T0 biofilm time point (Figure 2A).

Metabolic transitions accompanying different growth phases in planktonic cultures correlated with glucose availability. Glucose concentrations were measured by quantitative ^{1}H NMR for each sample at each time point; the values correspond to the extracellular glucose concentrations (mM) normalized to the viable cell counts (log or absolute number). TSB medium glucose concentration was measured to be 19.24 ± 0.99 mM. The transition from exponential growth to stationary phase was characterized by the complete exhaustion of glucose, which occurred within 8 h of inoculation (Figure 2B). During biofilm growth experiments both strains also exhibited nearly identical profiles for glucose consumption with the glucose being completely consumed within each 24 hour time point, that is, before the biofilm medium was refreshed (Figure 2B).

Both *S. aureus 10943* and *S. aureus 6538* planktonic cultures exhibited a drop in medium pH during exponential growth (Figure 2C). For example, the extracellular pH drops from pH 7.13 at inoculation to a pH of 5.21 at stationary phase and from pH 7.17 to pH 5.96 for *S. aureus 10943* and *S. aureus 6538*, respectively. In contrast with the planktonic cultures, the biofilm cultures exhibited increased bulk pH levels in the spent medium; the *S. aureus 10943* medium increased from an initial pH of 7.67 to pH 8.24 and *S. aureus 6538* medium increased from pH 7.18 to 7.99.

Intracellular and extracellular metabolites were identified and quantified for both *S. aureus 10943* and *S. aureus 6538* strains grown under planktonic and biofilm conditions. Samples were collected over an extended time course ranging from exponential growth to late-stationary phase for the planktonic cultures and every 24 hours, up to 72 h, for the biofilm cultures, which demonstrated a linear growth phenotype. Metabolism was quenched and metabolites extracted using an ice-cold aqueous methanol/sonification protocol, as described in the Experimental Procedures. Extracted metabolites were identified and quantified using 1D ^{1}H NMR, and NMR spectral features were assigned to particular metabolites by spectral pattern fitting to reference spectra of small-molecule metabolites annotated in the Chenomx (version 7.6) metabolomics database. Of the greater than 300 verified compounds in the Chenomx library, more than 120 water-soluble compounds from the sample supernatant and 40 water-soluble compounds

dx.doi.org/10.1021/pr500120c | *J. Proteome Res.* 2014, 13, 2973−2985

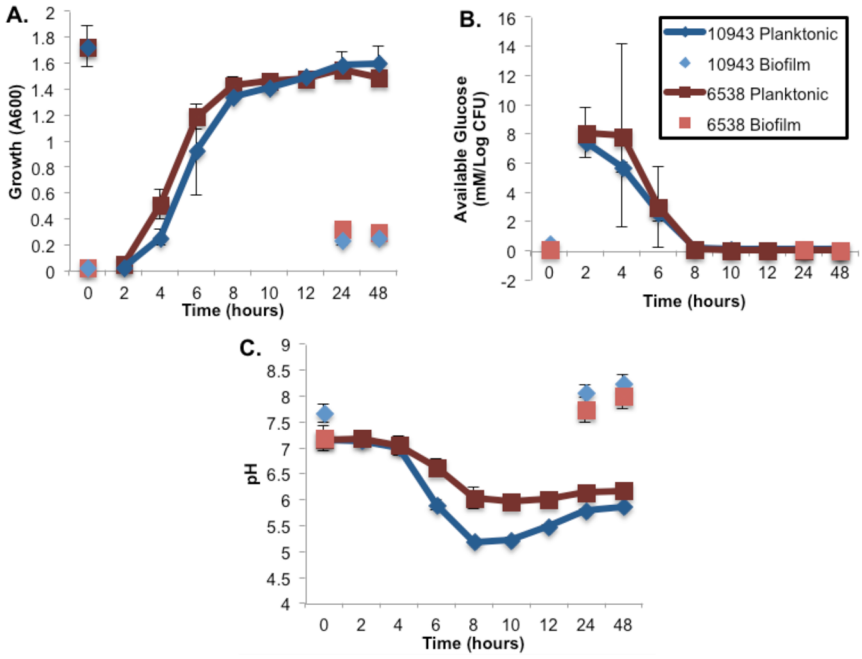

Figure 2. Changes in glucose concentration and pH in the bulk media correspond to transitions between growth phases in *S. aureus* cultures. (A) Growth curves for *S. aureus 6538* and *S. aureus 10943* planktonic and biofilm cultures were plotted for all growth time periods. Cultures were inoculated with an equal amount of cell mass, as determined by comparable absorbance readings of seed flasks (i.e., $OD_{600\ nm}$). Time zero refers to mature biofilms grown up to 72 h (T0) and inoculum for planktonic cultures, respectively. Error bars have been calculated from growth curve measurements of duplicate biological replicates for each growth condition and growth time point. (B) Decreasing glucose concentration in the media for planktonic cultures corresponds in time to transition from exponential to stationary phase of growth. For biofilm cultures, consumption of glucose is below the detection limit of ^{1}H 1D NMR for all time points of growth. (C) Changes in pH profile for planktonic cultures correspond in time to changes in growth rate, with significant pH differences between strains observed for biofilm cultures. Slight differences in bulk pH were detected between the two strains based on growth phase and growth phenotype.

from cell pellets were identified in at least one sample from at least one growth condition.

Differences in the two phylogenetically distinct *S. aureus* strains 10943 and 6538, grown both as biofilm cultures and planktonic cultures were distinguished based on PCA of their respective metabolite profiles. PCA utilizes orthogonal transformation of correlated metabolite profiles into linearly uncorrelated PCs to separate samples according to distinct patterns,[19] and provides a quantitative basis for distinguishing the *S. aureus* strains (Figure 3A–D). Both the MRSA (i.e., *S. aureus 10943*) and MSSA (i.e., *S. aureus 6538*) strains were separated along the principal component 1 (PC1) axis for both the intracellular and extracellular metabolite profiles of the planktonic cultures as well as the extracellular metabolite profiles of the biofilm cultures (Figure 3A–C, respectively). PC1 accounted for ~50% of the statistical variability within the samples, suggesting the two strains used distinguishably different metabolic strategies; however, the biofilm intracellular metabolite profiles clustered nearly identically (Figure 3D).

Quantitative Metabolite Profiles Can Distinguish between *S. aureus* Biofilm Growth and Planktonic Cell Cultures in Phylogenetically Distinct Strains of *S. aureus*

PCA comparison of both intracellular and extracellular metabolite profiles for both strains was analyzed concomitantly (Figures 4 and 5) to establish whether biofilm and planktonic phenotype of *S. aureus* can be quantitatively distinguished based on metabolic differences, irrespective of strains and growth stages (i.e., exponential, stationary, linear). PCA analysis of intracellular or extracellular metabolite profiles resulted in biofilm samples for both strains clustering into a single quadrant with no overlap of biofilm phenotype with planktonic phenotype (Figures 4 and 5). Because of biofilm metabolite profiles segregating into a single quadrant (lower, left quadrant, Figures 4 and 5), the combination of PC1 and PC2 identified those metabolites for which correlation coefficients are most significantly associated with the biofilm phenotype of *S. aureus* (Tables 1 and 2). As is conventional for many biological analyses, a 0.4 threshold for the correlation coefficients was used here to identify the most significant metabolite contributors to the PCA variations.[19] In addition, correlation coefficient values in bold indicate which metabolites are most significantly related to the PCs from which 2D PCA scores plot are built, further highlighting the statistical significance of these metabolites as contributing variables for sample distinction (Tables 1 and 2).

Amino acid profiles suggest that distinct selective amino acid uptake may be a key feature differentiating between biofilm and planktonic cultures in *S aureus*,[14] regardless of strain. Interestingly, PCA factor loadings analysis demonstrated that distinct amino acid profiles for both intracellular and extracellular pools of metabolites contribute significantly to the separation of the biofilm samples for both strains, including amines such as arginine (Table 1), hydroxy acids such serine (Table 1), amido acids such as asparagine (Tables 1 and 2), and aromatic amino acids such as histidine (Table 2). Arginine metabolism has been suggested to play an important role in biofilm survival,[14,21a] and the factor loadings analysis conducted here suggests that arginine catabolism is an important feature of the biofilm phenotype (Table 1). Indeed, amino acid catabolism may be a significant component of biofilm metabolism, as multiple metabolites associated with amino

dx.doi.org/10.1021/pr500120c | J. Proteome Res. 2014, 13, 2973–2985

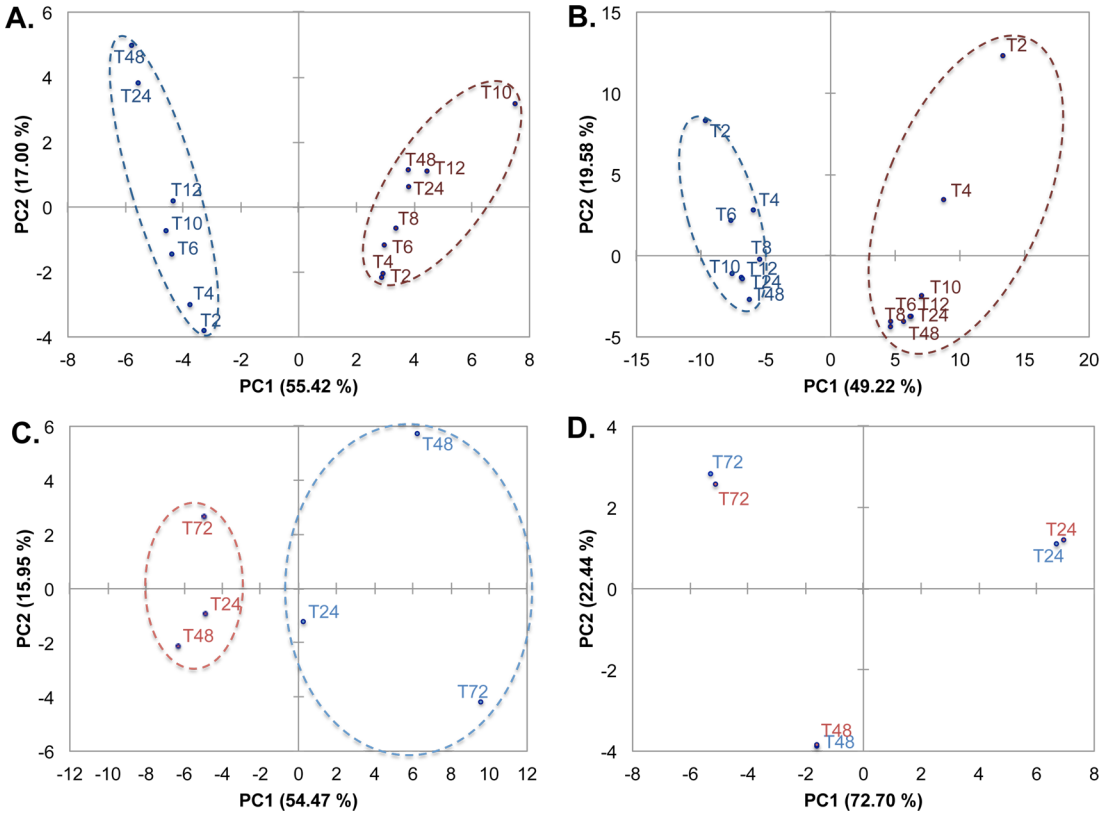

Figure 3. Principal component analysis (PCA) comparison of two *S. aureus* strains. 2D PCA scores plots indicate statistically significant sample separations along the first dimension (PC1) between the metabolite profiles of *S. aureus 10943* (blue lines) and *S. aureus 6538* (red lines) for both intracellular and extracellular metabolites of planktonic cultures (panels A and B, respectively) and biofilm extracellular metabolites (panel C, as detected by 1D ^{1}H NMR). In contrast, metabolite profiles for biofilm intracellular metabolites cluster nearly identically (panel D). Dark colors (red and blue) indicate planktonic cultures, and light colors (red and blue) indicate biofilm cultures. Numbers correspond to hours postinoculation for planktonic cultures (e.g., T2, T4, T6, etc.) and hours past reaching linear growth in biofilms (e.g., T24, T48, T72).

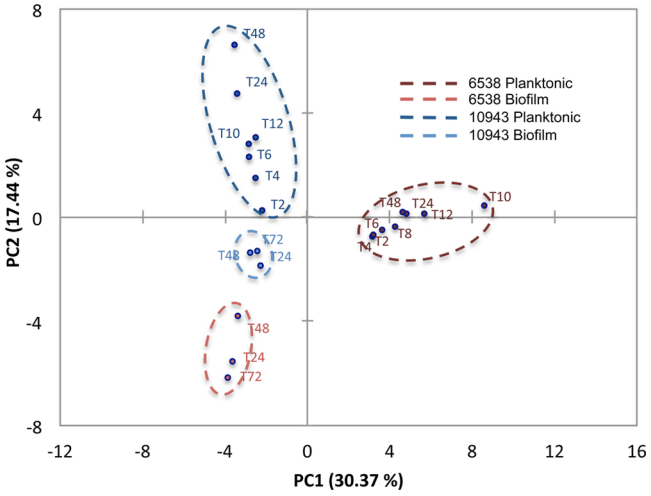

Figure 4. PCA analysis of intracellular metabolites for *S. aureus 10943* and *6538* biofilm and planktonic cultures results in statistical clustering of biofilm phenotype. PCA analysis of intracellular metabolites in *S. aureus 10943* and 6538 biofilm and planktonic cultures detected by 1D ^{1}H NMR separates the biofilm phenotype into a single quadrant of the 2D PCA scores plot as a result of significant statistical separations from *S. aureus 6538* planktonic cultures along PC1 and from *S. aureus 10943* planktonic cultures along PC2.

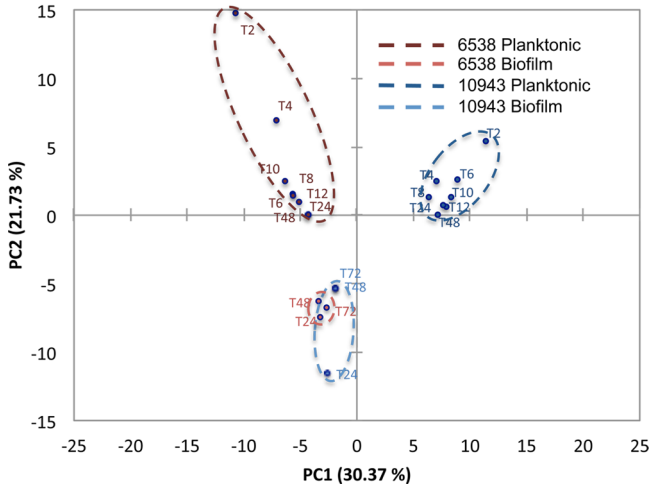

Figure 5. PCA analysis of extracellular metabolites for *S. aureus 10943* and *6538* biofilm and planktonic cultures results in statistical separation of the biofilm phenotype from its planktonic counterpart. PCA analysis of extracellular metabolite profiles in *S. aureus 10943* and 6538 biofilm and planktonic cultures detected by 1D ^{1}H NMR separates the biofilm phenotype into a single quadrant of the 2D PCA score plots as a result of statistically significant separations from *S. aureus 10943* planktonic cultures along PC1 and from *S. aureus 6538* planktonic cultures along PC2.

acid degradation contribute significantly to the statistical separation of the biofilm cultures in the PCA scores plots shown here, including metabolites associated with alanine, aspartate, cysteine, isoleucine, methionine, serine, threonine,

dx.doi.org/10.1021/pr500120c | *J. Proteome Res.* 2014, 13, 2973−2985

Table 1. Factor Analysis for Intracellular Metabolites

metabolite	correlation coefficient[a,b] PC1	PC2
acetate	**0.962**	−0.027
creatine	**0.961**	−0.038
caprylate	**0.955**	−0.024
acetone	**0.933**	−0.042
formate	**0.928**	−0.082
2-hydroxybutyrate	**0.876**	0.024
choline	**0.866**	0.084
betaine	**0.858**	0.156
acetoin	**-0.828**	0.124
lactate	**0.811**	0.023
methanol	**0.797**	−0.139
glutamate	**0.790**	0.023
alanine	**0.743**	0.232
ornithine	**0.725**	0.355
succinate	**-0.713**	0.237
aspartate	−0.584	−0.171
arginine	−0.458	**0.713**
acetoacetate	−0.450	−0.247
leucine	−0.442	**0.746**
glutamine	−0.433	**0.752**
creatinine	−0.389	**0.595**
isovalerate	−0.367	**-0.537**
2-hydroxyvalerate	−0.364	**-0.695**
glutarate	−0.361	0.569
3-hydroxybutyrate	−0.344	**−0.662**
4-aminobutyrate	−0.322	−0.581
isobutyrate	−0.322	−0.611
serine	−0.290	−0.512
cystathionine	−0.289	**0.631**
asparagine	−0.289	**0.629**
trans-aconitate	−0.285	**0.604**
threonate	−0.261	−0.439
propionate	−0.243	−0.481
2-hydroxyglutarate	−0.222	−0.466
creatine phosphate	−0.222	−0.466
isocitrate	−0.222	−0.466
sarcosine	−0.222	−0.466
succinylacetone	−0.222	−0.466
3-hydroxyphenylacetate	−0.203	**0.503**
acetamide	−0.203	**0.503**
percent total variance	30.37%	17.44%
cumulative percent variance		47.81%

[a]Significance of correlation coefficient set at threshold of 0.4. [b]Correlation coefficient numbers in bold indicate metabolites for which the statistical relatedness of the variable is most correlated to the PC, as indicated by the square of the cosine.

and histidine metabolic pathways (Tables 1 and 2). Whether *S. aureus* biofilms are selectively utilizing amino acids or catabolizing whichever small molecule is most available remains to be established. The PCA factor loadings analysis suggests that biofilms opt for the latter option because metabolites associated with catabolism of other amino acids, such as glycine, tryptophan, and lysine, do not contribute significantly to the separation of the biofilm samples on the PCA scores plots. (See Tables 1 and 2.)

Secondary energy sources also appear to be important to distinguishing the biofilm phenotype from its planktonic counterpart. Both intracellular and extracellular metabolites associated with lipid catabolism such as glycerol (Table 2), glycerate (Table 2), malonate (Table 2), and propionate (Table 1) contribute to the statistical separation of the biofilms into a single quadrant of the PCA scores plots. Malonate is also a product of pyrimidine degradation in some bacteria.[28] While genes for this pathway have been sequenced in staphylococcus species, a functional pathway has yet to be demonstrated; however, in support of a role for purine and pyrimidine catabolism in biofilm formation, multiple metabolites associated with catabolism of these molecules were identified as contributing to the discrimination between biofilm and planktonic phenotypes (Tables 1 and 2). In addition, pyrimidine nucleotides serve as precursors for synthesis of teichoic acids and peptidoglycan in *S. aureus*,[29] and may indicate biofilm metabolic investment in cell-wall synthesis and matrix deposition.

In addition, biofilms may effectively utilize alternative carbohydrate metabolic pathways once glucose has been consumed because hexose catabolism of galactose and mannose contributes to biofilm separation (Table 2). The correlation coefficient for acetoin indicates that this ketone contributes significantly to distinction between biofilms and planktonic cultures irrespective of *S. aureus* strains and highlights the importance of butanediol fermentation in biofilms, as has been suggested.[14]

Other studies have suggested that upregulation of glycolysis in biofilms is not directed toward production of energy but instead directs metabolic flux to other metabolic pathways engaged in the production of cell-wall components and matrix deposition.[12b] To this effect, correlation coefficients for metabolites associated with cell-wall synthesis such as *N*-acetylglutamine and UDP-*N*-acetylglucosamine are shown here to contribute significantly to segregating the biofilm samples into a single quadrant of the PCA scores plot (Figure 5).

S. aureus Biofilm Phenotype Is Distinguished Both by Adaptable Energy Production and Investment into Small Molecules Important for Sessile Survival

Using the information embedded in correlation coefficients of key metabolites, PCA score plots indicated which metabolic activities might most distinguish the biofilm phenotype from its planktonic counterpart (summarized in Figure 6). Glucose consumption by the biofilm suggests that while glucose is available, glycolysis is active (Figure 2B); however, once glucose is consumed, the biofilms appear to readily switch to alternative energy sources. As noted by others,[14] relatively high intracellular concentrations of acetoin, a metabolic precursor to 2,3-butanediol, indicate that butanediol fermentation is part of a mixed acid fermentation strategy employed by the biofilms. The fermentative metabolite profiles suggest that microaerobic and anaerobic environments exist within the biofilm, as has been previously suggested.[12a,b,14]

Also as previously reported,[14,21a] selective uptake of amino acids may differentiate between biofilm and planktonic cultures; however, in our study, the patterns of intracellular and extracellular amino acids are most significantly correlated with amino acid fermentation through the Stickland reaction,[30] in which one amino acid serves as an electron donor and one amino acid serves as an electron acceptor. For example, both *S. aureus 10943* and *S. aureus 6538* biofilms selectively transported isoleucine, an electron donor, into the cytosol, while concomitantly increasing intracellular pools of sarcosine, an electron acceptor, as well as secreting relatively high levels of

dx.doi.org/10.1021/pr500120c | J. Proteome Res. 2014, 13, 2973−2985

Table 2. Factor Analysis for Extracellular Metabolites

metabolite	correlation coefficient[a,b] PC1	PC2	metabolite	correlation coefficient[a,b] PC1	PC2
4-aminohippurate	**0.948**	0.259	trehalose	0.502	0.380
uridine	**0.947**	0.281	serotonin	0.474	0.049
choline	**0.947**	0.257	urea	0.468	0.071
2-hydroxybutyrate	**0.945**	0.273	N6-acetyllysine	0.465	0.044
isopropanol	**0.941**	0.267	isobutyrate	0.464	−0.242
GTP	**0.930**	0.268	glutarate	0.449	−0.258
5-hydroxyindole-3-acetate	**0.894**	0.292	asparagine	−0.446	**0.832**
isocaproate	**0.892**	0.206	alanine	−0.445	**0.849**
cysteine	**0.890**	0.288	nicotinurate	0.442	**0.766**
NADH	**0.887**	0.302	glycerol	−0.438	**0.828**
dimethylamine	**0.882**	0.274	threonine	−0.437	**0.742**
2′-deoxyinosine	**0.881**	0.265	*O*-phosphocholine	0.434	0.021
citrate	**0.880**	0.156	*sn*-glycero-3-phosphocholine	0.432	0.070
glycine	**0.878**	0.067	propylene glycol	−0.422	0.057
ethanolamine	**0.874**	0.296	2-hydroxyisobutyrate	−0.418	**0.789**
putrescine	**0.865**	0.225	serine	−0.396	**0.705**
AMP	**0.863**	0.081	lysine	0.387	**0.832**
2-aminobutyrate	**0.845**	0.198	thymine	0.381	**−0.523**
NADP+	**0.824**	0.206	leucine	−0.374	**0.862**
NADPH	**0.818**	0.276	glutamine	−0.349	**0.677**
sucrose	**0.817**	0.299	proline	−0.346	**0.672**
O-phosphoethanolamine	**0.816**	0.291	4-hydroxyphenyllactate	0.337	−0.437
arginine	**0.803**	0.038	aspartate	−0.326	**0.879**
nicotinate	**−0.803**	0.150	riboflavin	−0.307	**0.740**
creatinine	**0.801**	0.226	anserine	−0.249	0.539
methanol	**0.797**	0.252	phenylalanine	−0.238	**0.753**
myo-inositol	**0.792**	0.273	hypoxanthine	−0.229	**0.503**
O-acetylcholine	**0.788**	−0.027	tryptophan	0.221	**0.701**
carnitine	**0.781**	0.237	cystine	−0.210	**−0.632**
butyrate	**0.780**	0.264	glycerate	−0.205	**−0.680**
ethanol	**0.748**	0.186	phenylacetate	−0.203	**−0.636**
5-hydroxytryptophan	**−0.739**	0.603	*N*-acetylglucosamine	−0.202	−0.578
N-acetylserotonin	**0.723**	0.124	homocysteine	−0.200	−0.591
4-aminobutyrate	**−0.723**	0.552	2′-deoxyadenosine	−0.199	**0.757**
trimethylamine N-oxide	**0.719**	0.277	uracil	−0.196	**-0.540**
ATP	**0.710**	0.276	carnosine	−0.190	−0.543
oxypurinol	**0.698**	0.262	cystathionine	−0.184	−0.493
urocanate	**−0.692**	0.000	malonate	−0.182	−0.479
gluconate	**0.685**	0.134	maleate	0.116	**0.911**
betaine	**−0.675**	0.561	isovalerate	−0.114	**−0.666**
methionine	**−0.674**	0.552	*S*-adenosylhomocysteine	−0.110	**0.829**
creatine phosphate	**0.669**	0.160	valine	−0.107	0.516
glutathione	**0.662**	0.014	pyroglutamate	−0.096	**0.931**
sarcosine	**0.661**	0.071	biotin	−0.086	−0.463
glutamate	**0.655**	−0.026	2-phenylpropionate	−0.086	−0.463
pyridoxine	**−0.652**	0.627	galactose	−0.086	−0.463
pyruvate	−0.648	**0.656**	3-hydroxybutyrate	−0.086	−0.463
ornithine	**0.643**	0.113	4-pyridoxate	−0.086	−0.463
lactate	**0.643**	0.119	UDP-*N*-acetylglucosamine	−0.086	−0.463
succinate	**0.633**	0.122	2-hydroxy-3-methylvalerate	−0.086	−0.463
tyrosine	**−0.623**	0.266	3-aminoisobutyrate	−0.086	−0.463
ADP	0.607	0.067	mannose	−0.086	−0.463
O-phosphoserine	−0.598	**0.667**	nicotinic acid adenine dinucleotide	−0.086	−0.463
acetoin	−0.575	**0.672**	xanthosine	−0.086	−0.463
N-acetyltyrosine	0.560	0.055	6-hydroxynicotinate	−0.086	−0.463
melatonin	**0.559**	0.083	cholate	−0.086	−0.463
3-methylxanthine	0.551	0.209	galactitol	−0.086	−0.463
methylsuccinate	0.544	−0.029	*trans*-4-hydroxy-L-proline	−0.086	−0.463
isoleucine	−0.544	**0.719**	glucose	−0.070	**0.733**

dx.doi.org/10.1021/pr500120c | *J. Proteome Res.* 2014, 13, 2973−2985

Table 2. continued

metabolite	correlation coefficient[a,b] PC1	PC2	metabolite	correlation coefficient[a,b] PC1	PC2
histidine	−0.530	**0.595**	3-hydroxyisovalerate	0.033	**−0.618**
τ-methylhistidine	−0.529	**0.731**	adenosine	0.020	**0.673**
percent total variance				30.37%	21.73%
cumulative percent variance					52.10%

[a]Significance of correlation coefficient set at threshold of 0.4. [b]Correlation coefficient numbers in bold indicate metabolites for which the statistical relatedness of the variable is most correlated to the PC as indicated by the square of the cosine.

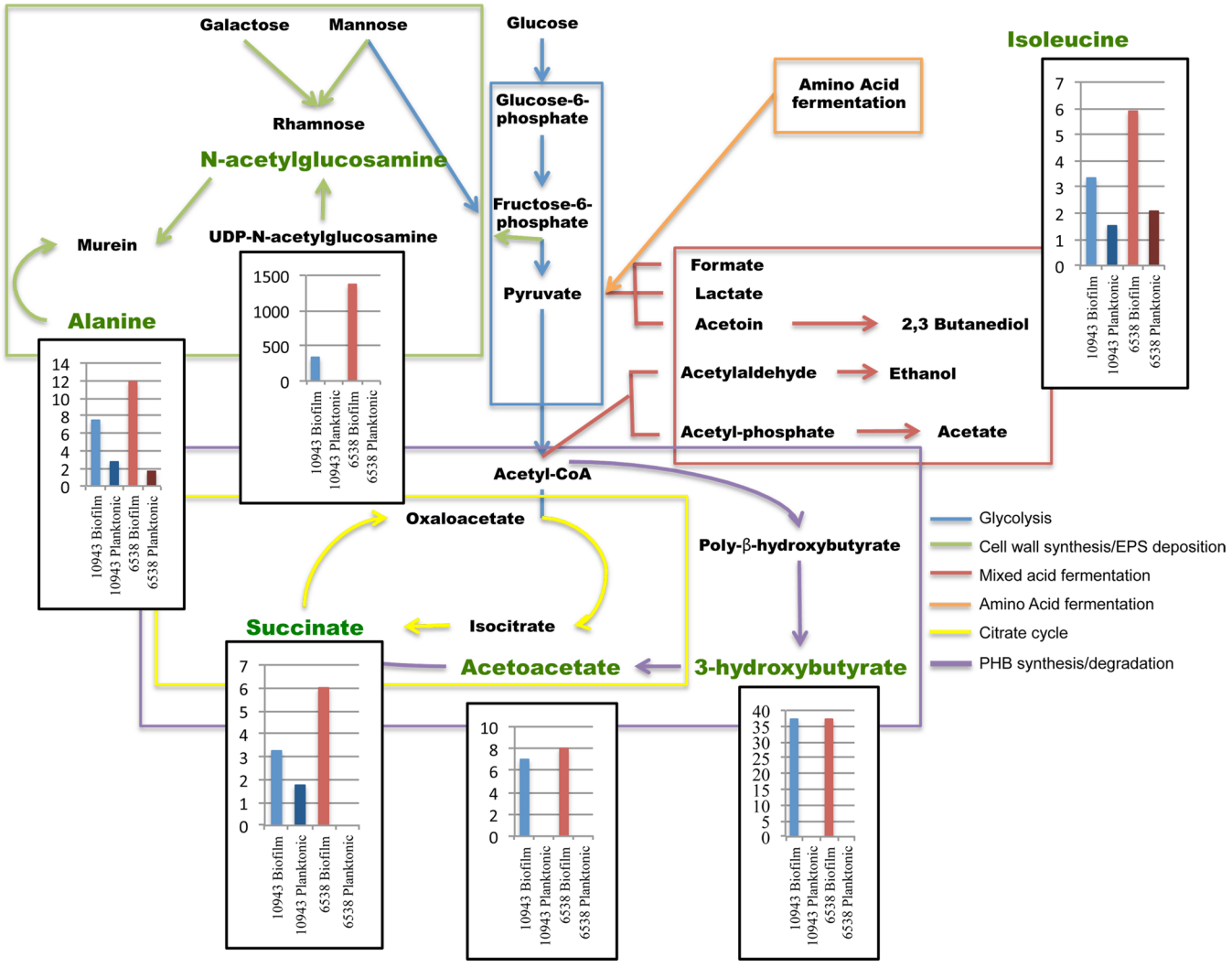

Figure 6. Schematic representation of central metabolism and secondary metabolic activity in *S. aureus* characteristic of the biofilm phenotype. Bar charts represent fold changes in metabolite concentrations for biofilm and stationary planktonic samples, respectively, normalized to the metabolite concentrations in each respective exponential planktonic culture for select intracellular and extracellular biofilm metabolites that contribute to statistical separation of the biofilm phenotype from the planktonic phenotype irrespective of strain. *S. aureus 10943* is indicated by blue bars and *S. aureus 6538* is indicated by red bars. Dark bars indicate planktonic samples and light bars indicate biofilm samples. Data shown are representative samples from duplicate experiments.

ammonia (data not shown), a byproduct of amino acid catabolism. This suggests that amino acid catabolism serves as an important source of energy for the biofilm phenotype and that amino acid uptake may not be specific, as previously suggested,[14] but rather is an adaptive strategy to environmental conditions and nutrient availability, a finding consistent with other data.[7]

It has been hypothesized that *S. aureus* biofilms adapt to strongly reduced conditions through production of reduced organic acids like lactate and alcohols including butanediol.[14] While butanediol fermentation was observed in both *S. aureus 10943* and *S. aureus 6538* biofilms (Figures 4 and 5), additional intracellular metabolites of importance to the PCA analysis included compounds associated with poly-*β*-hydroxybutyrate (PHB) synthesis and degradation.[31] To regulate NADH and NAD+ levels, PHB serves as both an electron and carbon sink in bacteria.[32] Relatively high intracellular pools of 3-hydroxybutyrate and acetoacetate, metabolites associated with

dx.doi.org/10.1021/pr500120c | J. Proteome Res. 2014, 13, 2973−2985

PHB synthesis and degradation, were measured as *S. aureus* maintains a favorable redox balance through appropriate NADH to NAD^+ ratios (Tables 1 and 2).

Finally, in the biofilm model used here,[17] the biofilms reach a linear phase and do not significantly increase in biomass over time (Figure 2A); however, the biofilms consume and secrete significant amounts of metabolites, suggesting a very dynamic metabolic state. As previously proposed, the output of this metabolic activity may be cell-wall synthesis in response to cellular turnover and deposition of EPS components.[12b,33] In support of this hypothesis, the PCA analyses shown here (Figures 4 and 5) indicate that alternative hexose utilization contributes significantly to the statistical separation of the biofilm and planktonic phenotypes. While hexose sugars can be catabolized via glycolysis, both mannose and galactose may be channeled into the production of rhamnose, a component found in exopolysaccharide repeating units.[34]

Cell-wall synthesis entails the building of murein monomers from precursors UDP-N-acetylglucosamine and UDP-*N*-acetylmuramate, both synthesized in the cytoplasm of *S. aureus*.[35] Both *N*-acetylglucosamine and its precursor UDP-*N*-acetylglucosamine were metabolites for which PCA correlation coefficients indicated that secretion of these metabolites is an important characteristic of both *S. aureus 10943* and *S. aureus 6538* biofilm phenotypes (Table 2). While selective uptake of alanine by the biofilms may be important for amino acid fermentation via the Stickland reactions, as previously mentioned, it may also play a significant role as a precursor for the synthesis of cell-wall components as well as EPS deposition. These results suggest that flexible metabolic activity specific to the biofilms not only includes the previously reported energy production from mixed acid fermentation and TCA activity but also involves significant energy expenditure for maintenance of a proper redox balance, synthesis of cell-wall components, and EPS matrix deposition (Figure 6).

DISCUSSION

Nonhealing of wounds such as diabetic and pressure ulcers is, in part, due to the persistence of bacterial biofilm-based infections;[4,10,36] however, metabolic contributions to persistence of the bacteria in the wound remain an area of investigation.[37] Specifically, there is interest in identifying small-molecule biomarkers that distinguish between biofilm and planktonic phenotypes, which could be used as a noninvasive, prognostic tool indicating bacterial biofilm colonization in a wound.[20b,36] In addition, such profiles could provide insights into physiological differences between biofilm and planktonic cell cultures, which could be exploited to therapeutic advantage. It has been speculated that pathogenicity in bacteria is the result of an evolutionary drive to obtain nutritional resources.[38] While traditional antibiotics have been designed against planktonically grown bacteria and to treat metabolically active bacteria, bacteria in a biofilm are metabolically different from planktonic bacteria;[39] therefore, the design of novel therapies for wounds necessitates considering and accounting for the unique ability of the biofilm to resist treatment, especially through adaptive metabolic changes. Because of the correlation between chronicity in wounds and bacterial biofilm contamination, a number of biofilm-targeted antimicrobials have emerged including the iron-binding innate immune molecule lactoferrin;[40] however, metabolic characterization of the biofilm phenotype has the potential to uncover many other biofilm-specific targets for the development of novel wound therapeutics.

Previous transcriptomics and proteomics analyses of *S. aureus* biofilm and planktonic cultures[12,14] demonstrated that, when grown as a biofilm, this facultative anaerobe switches to fermentative metabolism within the biofilm. Consistent with these observations, our data demonstrate that for both strains of *S. aureus* anaerobic metabolism is induced in the biofilm cultures and suggest that mixed acid fermentation is active, contributing to a biomarker profile that distinguishes between biofilm and planktonic phenotypes.

Selective amino acid uptake profiles have been reported for *S. aureus* biofilm cultures when compared to planktonic cultures.[14,21a] While statistical PCA analysis of the biofilm and planktonic cultures did identify both intracellular and extracellular metabolite patterns that distinguished between the biofilm and planktonic phenotypes, regardless of strain type, these profiles did not exactly match those previously reported.[14,21a] Whereas Zhu and coworkers[14] reported selective uptake of glutamine, serine, proline, glycine, threonine, and arginine, and Wu and coworkers[21a] reported selective uptake of arginine, we observed metabolite trends that distinguish between biofilm and planktonic phenotype based on differential intracellular pools of arginine, aspartate, glutamine, leucine, and serine and extracellular pools of alanine, asparagine, histidine, isoleucine, methionine, threonine, and tyrosine. These results suggest that while amino acid metabolism by the biofilm is important, the specific profile of amino acids transported into the cytosol is not a discriminant in and of itself of biofilm versus planktonic modes of growth.

Metabolic discrimination of biofilms independent of strain type is due in part to different intracellular concentrations of amino acids that function as electron donors (alanine, leucine, isoleucine, histidine) and electron acceptors (leucine and sarcosine) for amino acid fermentation by the Stickland reaction.[30] These data suggest that while selective amino acid uptake profiles do indicate significant amino acid utilization by *S. aureus* in response to redox needs, these profiles may not be specific to any particular set of amino acids and may rather reflect the opportunistic scavenging of the bacteria for whichever electron donor or acceptors may most readily be available.

Furthermore, metabolic discrimination of biofilms as established by PCA analysis of different metabolite expression patterns suggests that *S. aureus* biofilms might utilize secondary metabolic pathways to address redox stress. For example, when oxygen is limited, the synthesis of poly-β-hydroxybutyrate (PHB) could serve as an efficient electron sink. Degradation of PHB would contribute to cellular redox balance by reducing NAD^+ to NADH concomitantly with the breakdown of PHB to acetoacetate and entry of acetate into the TCA cycle (Figure 6). Although PHB was detected in *S. aureus* nearly 50 years ago,[41] the complete metabolic pathway for both synthesis and degradation of this polymer has yet to be firmly established in *S. aureus*. Putative *S. aureus* genes for PHB biosynthesis and degradation have been identified and annotated to be associated with virulence; however, demonstration of a functional PHB metabolic pathway in *S. aureus* remains to be accomplished.[42] The question of whether *S. aureus* biofilms selectively utilize this pathway as a mechanism to maintain an appropriate intracellular redox balance warrants further investigation.

Consistent with previous observations,[12a,b] metabolic investment in synthesis of cell-wall components and EPS deposition contributes significantly to the statistical separation of the biofilm and planktonic phenotypes in the PCA analysis (Figures 4 and 5). Despite having reached linear growth phase, the biofilm cultures exhibit significant central metabolism activity without a significant increase in the number of viable cells. Strain-independent PCA statistical grouping of metabolite variables characteristic of the biofilm phenotype identified metabolites associated with alternative hexose utilization, suggesting that rhamnose incorporation into EPS may be important for the *S. aureus* biofilm mode of growth. While rhamnose incorporation into the EPS is important for the common wound colonizer *Pseudomonas aeruginosa*[43] and rhamnose synthesis may occur in *S. aureus*, the intricacies of hexose metabolism in *S. aureus* have yet to be dissected. In contrast, cell-wall synthesis metabolism is well established in *S. aureus*, and in this study precursor metabolites were shown to significantly contribute to the distinctive characteristics of the biofilm phenotype compared with its planktonic counterpart in a strain-independent manner. Whether this metabolic investment indicates static, viable cell turnover within the biofilm or some strategy for biofilm persistence is a question of significant clinical interest, especially considering that cell-wall teichoic acids play a major role in host–pathogen interactions[44] and alterations in cell-wall components can significantly affect microbial susceptibility to antibiotics and cell-wall disrupting agents.[33]

■ CONCLUSIONS

While identification of a single, robust small molecule biomarker that distinguishes between biofilm and planktonic cultures would have significant translational research appeal for clinical diagnostics, it is unlikely that such a universal metabolite biomarker exists despite encouraging data to the contrary.[20b] Indeed, the NMR metabolomics analysis presented here indicates that even within a single bacterial species significant differences in metabolite patterns can be observed for both biofilm and planktonic phenotypes. Despite the complexity of such an analysis and by using a comprehensive experimental approach that included phylogenetically distinct strains of *S. aureus* and metabolite sampling through time courses that account for multiple growth phases, we have demonstrated herein the ability to distinguish biofilm from planktonic cultures based on distinct metabolite profiles. While the NMR metabolomics approach presented is robust, the research strategy incorporated only two strains of a single species; it will be of significant interest to explore whether comparable metabolite profile analyses can distinguish between biofilms and planktonic cultures of other Gram-positive opportunistic pathogens, as well as Gram-negative pathogens and potentially mixed species biofilms. In addition to demonstrating the use of global metabolite profiling for discriminating between *S. aureus* biofilm and planktonic cultures, the contribution of metabolite variables to the statistical separation of the biofilm phenotype from its planktonic counterpart in the PCA analyses presented here sheds light on some tantalizing areas of bacterial metabolism for further investigation and indicates how little is known about the physiology and metabolic characteristics of this important common, opportunistic pathogen.

■ AUTHOR INFORMATION

Corresponding Authors

*M.C.B.A.: Tel: (406) 994-6838. Fax: (406) 994-4801. E-mail. mcammons@chemistry.montana.edu.
*V.C.: Tel: (406) 994-7244. Fax: (406) 994-4801. E-mail: vcopie@chemistry.montana.edu.

Notes

The authors declare no competing financial interest.

■ ACKNOWLEDGMENTS

Cultures of *S. aureus 10943* and *S. aureus 6538* were kindly provided by the Center for Biofilm Engineering at Montana State University. This research was supported, in part, by NIH grant 3P20GM103394–05S1, a supplement to parent grant 8P20GM103394–05 (M.C.B.A., R.P.C., and V.C.), NIH grant 1KO1GM103821–01 (to M.C.B.A.), NIH grant 1RO3AR060995-01A1 (to K.R.K. and M.C.B.A.), and a Howard Hughes Medical Institute (HHMI) Undergraduate Fellowship (to M.A.G.). The NMR metabolomics experiments were performed at MSU on a 600 MHz solution NMR spectrometer purchased in part, and recently upgraded to an AVANCE III console and TCI cryoprobe, with funds from NIH grants 1-S10RR13878–01 and S10RR026659-01A1. The content is solely the responsibility of the authors and does not necessarily represent the official views of the NIH.

■ ABBREVIATIONS

CA-MRSA, community-acquired methicillin-resistant *Staphylococcus aureus*; DSS, 4,4-dimethyl-4-silapentane-1-sulfonic acid; EPS, extracellular polymeric substance; MRSA, methicillin-resistant *Staphylococcus aureus*; MSSA, methicillin-susceptible *Staphylococcus aureus*; NOESY, nuclear Overhauser enhancement spectroscopy; PC, principal component; PCA, principal component analysis; PHB, poly-β-hydroxybutyrate; TCA, tricarboxylic acid; TSB, tryptic soy broth

■ REFERENCES

(1) American Diabetes Association.. conomic costs of diabetes in the U.S In 2007. *Diabetes Care* **2008**, *31* (3), 596–615.
(2) James, G. A.; Swogger, E.; Wolcott, R.; Pulcini, E.; Secor, P.; Sestrich, J.; Costerton, J. W.; Stewart, P. S. Biofilms in chronic wounds. *Wound Repair Regener.* **2008**, *16* (1), 37–44.
(3) (a) Konturek, P. C.; Brzozowski, T.; Konturek, S. J.; Kwiecien, S.; Dembinski, A.; Hahn, E. G. Influence of bacterial lipopolysaccharide on healing of chronic experimental ulcer in rat. *Scand. J. Gastroenterol.* **2001**, *36* (12), 1239–1247. (b) Power, C.; Wang, J. H.; Sookhai, S.; Street, J. T.; Redmond, H. P. Bacterial wall products induce downregulation of vascular endothelial growth factor receptors on endothelial cells via a CD14-dependent mechanism: implications for surgical wound healing. *J. Surg. Res.* **2001**, *101* (2), 138–145.
(4) Costerton, J. W.; Stewart, P. S.; Greenberg, E. P. Bacterial biofilms: a common cause of persistent infections. *Science* **1999**, *284* (5418), 1318–1322.
(5) Dowd, S. E.; Sun, Y.; Secor, P. R.; Rhoads, D. D.; Wolcott, B. M.; James, G. A.; Wolcott, R. D. Survey of bacterial diversity in chronic wounds using pyrosequencing, DGGE, and full ribosome shotgun sequencing. *BMC Microbiol.* **2008**, *8*, 43.
(6) (a) Burke, K. A.; Lascelles, J. Nitrate reductase system in Staphylococcus aureus wild type and mutants. *J. Bacteriol.* **1975**, *123* (1), 308–316. (b) Evans, J. B. Uracil and pyruvate requirements of anaerobic growth of staphylococci. *J. Clin. Microbiol.* **1975**, *2* (1), 14–17. (c) Strasters, K. C.; Winkler, K. C. Carbohydrate Metabolism of Staphylococcus Aureus. *J. Gen. Microbiol.* **1963**, *33*, 213–229.

(7) Leibig, M.; Liebeke, M.; Mader, D.; Lalk, M.; Peschel, A.; Gotz, F. Pyruvate formate lyase acts as a formate supplier for metabolic processes during anaerobiosis in Staphylococcus aureus. *J. Bacteriol.* **2011**, *193* (4), 952−962.
(8) (a) Stewart, P. S.; Franklin, M. J. Physiological heterogeneity in biofilms. *Nat. Rev. Microbiol.* **2008**, *6* (3), 199−210. (b) Rasmussen, K.; Lewandowski, Z. Microelectrode measurements of local mass transport rates in heterogeneous biofilms. *Biotechnol. Bioeng.* **1998**, *59* (3), 302−309.
(9) (a) Fuchs, S.; Pane-Farre, J.; Kohler, C.; Hecker, M.; Engelmann, S. Anaerobic gene expression in Staphylococcus aureus. *J. Bacteriol.* **2007**, *189* (11), 4275−89. (b) Bowden, G. H.; Li, Y. H. Nutritional influences on biofilm development. *Adv. Dental Res.* **1997**, *11* (1), 81−99.
(10) Stewart, P. S. Mechanisms of antibiotic resistance in bacterial biofilms. *Int. J. Med. Microbiol.* **2002**, *292* (2), 107−113.
(11) Gilbert, P.; Brown, M. R. Biofilms and beta-lactam activity. *J. Antimicrob. Chemother.* **1998**, *41* (5), 571−572.
(12) (a) Resch, A.; Rosenstein, R.; Nerz, C.; Gotz, F. Differential gene expression profiling of Staphylococcus aureus cultivated under biofilm and planktonic conditions. *Appl. Environ. Microbiol.* **2005**, *71* (5), 2663−2676. (b) Resch, A.; Leicht, S.; Saric, M.; Pasztor, L.; Jakob, A.; Gotz, F.; Nordheim, A. Comparative proteome analysis of Staphylococcus aureus biofilm and planktonic cells and correlation with transcriptome profiling. *Proteomics* **2006**, *6* (6), 1867−1877. (c) Beenken, K. E.; Dunman, P. M.; McAleese, F.; Macapagal, D.; Murphy, E.; Projan, S. J.; Blevins, J. S.; Smeltzer, M. S. Global gene expression in Staphylococcus aureus biofilms. *J. Bacteriol.* **2004**, *186* (14), 4665−4684.
(13) Hollywood, K.; Brison, D. R.; Goodacre, R. Metabolomics: current technologies and future trends. *Proteomics* **2006**, *6* (17), 4716−4723.
(14) Zhu, Y.; Weiss, E. C.; Otto, M.; Fey, P. D.; Smeltzer, M. S.; Somerville, G. A. Staphylococcus aureus biofilm metabolism and the influence of arginine on polysaccharide intercellular adhesin synthesis, biofilm formation, and pathogenesis. *Infect. Immun.* **2007**, *75* (9), 4219−4226.
(15) Becher, D.; Hempel, K.; Sievers, S.; Zuhlke, D.; Pane-Farre, J.; Otto, A.; Fuchs, S.; Albrecht, D.; Bernhardt, J.; Engelmann, S.; Volker, U.; van Dijl, J. M.; Hecker, M. A proteomic view of an important human pathogen−towards the quantification of the entire Staphylococcus aureus proteome. *PloS One* **2009**, *4* (12), e8176.
(16) (a) Beenken, K. E.; Blevins, J. S.; Smeltzer, M. S. Mutation of sarA in Staphylococcus aureus limits biofilm formation. *Infect. Immun.* **2003**, *71* (7), 4206−4211. (b) Cramton, S. E.; Gerke, C.; Schnell, N. F.; Nichols, W. W.; Gotz, F. The intercellular adhesion (ica) locus is present in Staphylococcus aureus and is required for biofilm formation. *Infect. Immun.* **1999**, *67* (10), 5427−5433. (c) Rohde, H.; Knobloch, J. K.; Horstkotte, M. A.; Mack, D. Correlation of biofilm expression types of Staphylococcus epidermidis with polysaccharide intercellular adhesin synthesis: evidence for involvement of icaADBC genotype-independent factors. *Med. Microbiol. Immunol.* **2001**, *190* (3), 105−112.
(17) Kirker, K. R.; Secor, P. R.; James, G. A.; Fleckman, P.; Olerud, J. E.; Stewart, P. S. Loss of viability and induction of apoptosis in human keratinocytes exposed to Staphylococcus aureus biofilms in vitro. *Wound Repair Regener.* **2009**, *17* (5), 690−699.
(18) Wishart, D. S. Quantitative metabolomics using NMR. *TrAC, Trends Anal. Chem.* **2008**, *27* (3), 228−237.
(19) Jackson, J. E. *A User's Guide to Principal Components*; Wiley-Interscience: Hoboken, NJ, 2003; p xvii, 569 p.
(20) (a) Lipp, C.; Kirker, K.; Agostinho, A.; James, G.; Stewart, P. Testing wound dressings using an in vitro wound model. *J. Wound Care* **2010**, *19* (6), 220−226. (b) Secor, P. R.; Jennings, L. K.; James, G. A.; Kirker, K. R.; Pulcini, E. D.; McInnerney, K.; Gerlach, R.; Livinghouse, T.; Hilmer, J. K.; Bothner, B.; Fleckman, P.; Olerud, J. E.; Stewart, P. S. Phevalin (aureusimine B) production by Staphylococcus aureus biofilm and impacts on human keratinocyte gene expression. *PloS One* **2012**, *7* (7), e40973. (c) Secor, P. R.; James, G. A.; Fleckman, P.; Olerud, J. E.; McInnerney, K.; Stewart, P. S. Staphylococcus aureus Biofilm and Planktonic cultures differentially impact gene expression, mapk phosphorylation, and cytokine production in human keratinocytes. *BMC Microbiol.* **2011**, *11*, 143. (d) Kirker, K. R.; James, G. A.; Fleckman, P.; Olerud, J. E.; Stewart, P. S. Differential effects of planktonic and biofilm MRSA on human fibroblasts. *Wound Repair Regener.* **2012**, *20* (2), 253−261.
(21) (a) Wu, X. H.; Yu, H. L.; Ba, Z. Y.; Chen, J. Y.; Sun, H. G.; Han, B. Z. Sampling methods for NMR-based metabolomics of Staphylococcus aureus. *Biotechnol. J.* **2010**, *5* (1), 75−84. (b) Sun, J. L.; Zhang, S. K.; Chen, J. Y.; Han, B. Z. Metabolic profiling of Staphylococcus aureus cultivated under aerobic and anaerobic conditions with (1)H NMR-based nontargeted analysis. *Can. J. Microbiol.* **2012**, *58* (6), 709−718.
(22) (a) Faijes, M.; Mars, A. E.; Smid, E. J. Comparison of quenching and extraction methodologies for metabolome analysis of Lactobacillus plantarum. *Microb. Cell Fact.* **2007**, *6*, 27. (b) Hiller, J.; Franco-Lara, E.; Papaioannou, V.; Weuster-Botz, D. Fast sampling and quenching procedures for microbial metabolic profiling. *Biotechnol. Lett.* **2007**, *29* (8), 1161−1167.
(23) (a) Taymaz-Nikerel, H.; de Mey, M.; Ras, C.; ten Pierick, A.; Seifar, R. M.; van Dam, J. C.; Heijnen, J. J.; van Gulik, W. M. Development and application of a differential method for reliable metabolome analysis in Escherichia coli. *Anal. Biochem.* **2009**, *386* (1), 9−19. (b) Villas-Boas, S. G.; Bruheim, P. Cold glycerol-saline: the promising quenching solution for accurate intracellular metabolite analysis of microbial cells. *Anal. Biochem.* **2007**, *370* (1), 87−97. (c) Villas-Boas, S. G.; Hojer-Pedersen, J.; Akesson, M.; Smedsgaard, J.; Nielsen, J. Global metabolite analysis of yeast: evaluation of sample preparation methods. *Yeast* **2005**, *22* (14), 1155−1169. (d) Wittmann, C.; Kromer, J. O.; Kiefer, P.; Binz, T.; Heinzle, E. Impact of the cold shock phenomenon on quantification of intracellular metabolites in bacteria. *Anal. Biochem.* **2004**, *327* (1), 135−139.
(24) (a) Weljie, A. M.; Newton, J.; Mercier, P.; Carlson, E.; Slupsky, C. M. Targeted profiling: quantitative analysis of 1H NMR metabolomics data. *Anal. Chem.* **2006**, *78* (13), 4430−4442. (b) Tredwell, G. D.; Edwards-Jones, B.; Leak, D. J.; Bundy, J. G. The development of metabolomic sampling procedures for Pichia pastoris, and baseline metabolome data. *PloS One* **2011**, *6* (1), e16286.
(25) Worley, B.; Powers, R. Multivariate Analysis in Metabolomics. *Curr. Metabolomics* **2013**, *1* (1), 92−107.
(26) Gillespie, J. J.; Wattam, A. R.; Cammer, S. A.; Gabbard, J. L.; Shukla, M. P.; Dalay, O.; Driscoll, T.; Hix, D.; Mane, S. P.; Mao, C.; Nordberg, E. K.; Scott, M.; Schulman, J. R.; Snyder, E. E.; Sullivan, D. E.; Wang, C.; Warren, A.; Williams, K. P.; Xue, T.; Yoo, H. S.; Zhang, C.; Zhang, Y.; Will, R.; Kenyon, R. W.; Sobral, B. W. PATRIC: the comprehensive bacterial bioinformatics resource with a focus on human pathogenic species. *Infect. Immun.* **2011**, *79* (11), 4286−4298.
(27) Liu, G. Y.; Essex, A.; Buchanan, J. T.; Datta, V.; Hoffman, H. M.; Bastian, J. F.; Fierer, J.; Nizet, V. Staphylococcus aureus golden pigment impairs neutrophil killing and promotes virulence through its antioxidant activity. *J. Exp. Med.* **2005**, *202* (2), 209−215.
(28) Kim, Y. S. Malonate metabolism: biochemistry, molecular biology, physiology, and industrial application. *J. Biochem. Mol. Biol.* **2002**, *35* (5), 443−451.
(29) Liebeke, M.; Dorries, K.; Zuhlke, D.; Bernhardt, J.; Fuchs, S.; Pane-Farre, J.; Engelmann, S.; Volker, U.; Bode, R.; Dandekar, T.; Lindequist, U.; Hecker, M.; Lalk, M. A metabolomics and proteomics study of the adaptation of Staphylococcus aureus to glucose starvation. *Mol. Biosyst.* **2011**, *7* (4), 1241−1253.
(30) Nisman, B. The Stickland reaction. *Bacteriol. Rev.* **1954**, *18* (1), 16−42.
(31) Dawes, E. A. *Microbial Energetics*; Blackie: New York, 1986; p viii, 187 p.
(32) Khosravi-Darani, K.; Mokhtari, Z. B.; Amai, T.; Tanaka, K. Microbial production of poly(hydroxybutyrate) from C(1) carbon sources. *Appl. Microbiol. Biotechnol.* **2013**, *97* (4), 1407−1424.
(33) Liebeke, M.; Meyer, H.; Donat, S.; Ohlsen, K.; Lalk, M. A metabolomic view of Staphylococcus aureus and its ser/thr kinase and

phosphatase deletion mutants: involvement in cell wall biosynthesis. *Chem. Biol.* **2010**, *17* (8), 820−830.
(34) Welman, A. D.; Maddox, I. S. Exopolysaccharides from lactic acid bacteria: perspectives and challenges. *Trends Biotechnol.* **2003**, *21* (6), 269−274.
(35) Navarre, W. W.; Schneewind, O. Surface proteins of gram-positive bacteria and mechanisms of their targeting to the cell wall envelope. *Microbiol. Mol. Biol. Rev.* **1999**, *63* (1), 174−229.
(36) Ammons, M. C. Anti-biofilm strategies and the need for innovations in wound care. *Recent Pat. Anti-Infect. Drug Discovery* **2010**, *5* (1), 10−17.
(37) Mah, T. F. Biofilm-specific antibiotic resistance. *Future Microbiol.* **2012**, *7* (9), 1061−1072.
(38) Rohmer, L.; Hocquet, D.; Miller, S. I. Are pathogenic bacteria just looking for food? Metabolism and microbial pathogenesis. *Trends Microbiol.* **2011**, *19* (7), 341−348.
(39) Davey, M. E.; O'Toole G, A. Microbial biofilms: from ecology to molecular genetics. *Microbiol Mol. Biol. Rev.* **2000**, *64* (4), 847−867.
(40) Ammons, M. C.; Ward, L. S.; Fisher, S. T.; Wolcott, R. D.; James, G. A. In vitro susceptibility of established biofilms composed of a clinical wound isolate of Pseudomonas aeruginosa treated with lactoferrin and xylitol. *Int. J. Antimicrob. Agents* **2009**, *33* (3), 230−236.
(41) Ivler, D. Comparative metabolism of virulent and avirulent staphylococci. *Ann. N.Y. Acad. Sci.* **1965**, *128*, 62−80.
(42) (a) Uhlemann, A. C.; Porcella, S. F.; Trivedi, S.; Sullivan, S. B.; Hafer, C.; Kennedy, A. D.; Barbian, K. D.; McCarthy, A. J.; Street, C.; Hirschberg, D. L.; Lipkin, W. I.; Lindsay, J. A.; DeLeo, F. R.; Lowy, F. D. Identification of a highly transmissible animal-independent Staphylococcus aureus ST398 clone with distinct genomic and cell adhesion properties. *mBio* **2012**, *3*, 2. (b) Szewczyk, E.; Mikucki, J. Poly-beta-hydroxybutyric acid in staphylococci. *FEMS Microbiol. Lett.* **1989**, *52* (3), 279−284.
(43) Wozniak, D. J.; Wyckoff, T. J.; Starkey, M.; Keyser, R.; Azadi, P.; O'Toole, G. A.; Parsek, M. R. Alginate is not a significant component of the extracellular polysaccharide matrix of PA14 and PAO1 Pseudomonas aeruginosa biofilms. *Proc. Natl. Acad. Sci. U.S.A.* **2003**, *100* (13), 7907−7912.
(44) Weidenmaier, C.; Peschel, A. Teichoic acids and related cell-wall glycopolymers in Gram-positive physiology and host interactions. *Nat. Rev. Microbiol.* **2008**, *6* (4), 276−287.